Available online at www.garmian.edu.krd

Passer Journal

Passer 5 (Issue 1) (2023) 46-51

http://passer.garmian.edu.krd/

A DFT study of structural, electronic, and optical properties of Lead-free and Ge-based cubic perovskite $RbGeX_3$ (X= I, Br and Cl)

Nawzad Abdullah Abdulkareem[1*]

[1]*Theoretical Physics Group, Department of Physics, Faculty of Science, University of Zakho, Kurdistan Region, Iraq.*

Received 20 November 2022; revised 04 January 2023;
accepted 05 January 2023; available online 14 January 2023

DOI: 10.24271/PSR.2023.371069.1187

ABSTRACT

The current research uses density functional theory (DFT) approximations in conjunction with the plane wave-pseudopotential method to investigate structural, electronic, and optical properties of Pb-free cubic perovskite $RbGeX_3$ (X= I, Br and Cl) materials. More specifically, Norm-conserving pseudopotential has been employed to describe the ion and valence electrons interaction, and GGA-PBE flavor is used to represent the exchange-correlation part of the energy of the GGA approximation. Lattice parameters obtained are 5.95, 5.55, and 5.29 Å for $RbGeX_3$ (where X=I, Br, and Cl), respectively, and they are comparable with available empirical and other values. The direct band gap nature of the three compounds under research here is shown and our values of the band gap energy E_g are agree with the other available results. Materials under research show responses to electromagnetic radiation starting from the infrared region to very high energies (~ 33 eV). The $RbGeI_3$ has the lowest E_g value at the low region energies and the highest optical response peaks but $RbGeCl_3$ has the highest optical response peaks at energies located near ~20 eV. Our results show that these materials are good candidates for photo electronic applications including solar cells

Keywords: Pb-free perovskites, $RbGeX_3$ (X= I, Br and Cl), DFT, electronic properties, optical properties, ABINIT.

1. Introduction

Perovskite materials are intensively under research and they are promising materials for a variety of photo optic applications because they have a tunable band gap due to the various elements which can be used to fabricate these materials[1-4]. These materials have been used to fabricate light-emitting diodes (LED) and photodetectors[5-8]. In the last decade, researchers have shown the potential of the organic-inorganic and all inorganic Pb-based perovskite materials for the next generation, low-cost solar cell. The efficiency of perovskite-based solar cells has increased dramatically up to 25.2% in 12 years[9]. The general formula of the halide perovskite is described as ABX_3, where A, B, and X are an organic or inorganic cation, a metal cation, and a halogen anion, respectively[10-13]. Lead replaced B in perovskites which contain the Pb element[14-18]. An issue here remains because of the toxicity of the Pb element. Researchers are trying intensively to fabricate and study an efficient solar cell from Pb-free perovskite material[19-28]. The toxicity issue can be dealt with by removing Pb and substituting an element such as tin (Sn) and germanium (Ge)[29-33].

Among Pb-free perovskites, Ge-based perovskites have significance in different applications including solar cells. Electronic properties are calculated by synthesizing $AGeI_3$ (where A= CH_3NH_3, $HC(NH_2)_2$, $CH_3C(NH_2)_2$, $C(NH_2)_3$, $(CH_3)_3NH$ and $(CH_3)_2C(H)NH_3$)[34], it is shown that they have direct band gap and in the visible range spectrum. A highly luminescent (Up to 71%) Ge–Pb perovskite film with photoluminescence quantum efficiencies has been studied, and a new method is proposed for the eco-friendly light emitted technique[35]. A computational calculation combined with an experiment has confirmed that AGeI3 (A=Cs, CH_3NH_3 or $HC(NH_2)_2$) has strong potential for future solar cells[36]. However, Ge-based solar cell has low power conversion and it has to be improved. The power efficiency is improved up to 0.57% for $MAGeI_{2.7}Br_{0.3}$.

Organic cations as long as Cesium (Cs) can be replaced by Rb due to their similarity in electronic properties and their location in the periodic table. Recently researchers have investigated $RbGeX_3$ (where X= I, Br, and Cl) computationally and experimentally to provide more information on Ge-based perovskites. Density functional calculations have been performed to investigate structural, elastic, electronic, and optical properties of inorganic Ge-based perovskite with rhombohedral structure (space group R3m) and cubic structure with space group Fm-3m, Results confirmed these compounds have a wide range of absorption in the visible and ultraviolet energy values which

* Corresponding author
E-mail address: nawzad.abdulkareem@uoz.edu.krd (Instructor).
Peer-reviewed under the responsibility of the University of Garmian.

confirms their future role in various optoelectronic applications and they are strong candidates for the future solar cell[32, 37]. Specially $RbGeI_3$ has the ability for harvesting maximum photon energies in IR and UV spectra[38].

Due to our perspective, more investigation is demanded to confirm findings on $RbGeX_3$ (where X= I, Br, and Cl). In the current work, structural, and optoelectronic properties are studied for the Ge-based $RbGeX_3$ (where X=I, Br, and Cl) in cubic structure (space group 221) using PBE-GGA and density fictional perturbation theory (DFPT) approximation.

2. Computational Methodology

In this research, structural properties, electronic properties, and optic response to electromagnetic radiation have been calculated in the framework of density functional theory (DFT)[39, 40]. For optic properties, Eigen values and Eigen functions resulted from density functional perturbation theory (DFPT) calculations used in Kramers-Kronig relations[41]. All calculations have been performed with approximations implemented in ABINIT software[42].

Pseudopotential as core-valence states interaction and plane-wave as basis sets are chosen to perform calculations. Pseudopotentials used here are previously generated by M.Krack where Goedecker, Teter, and Hutter (GTH) approach was used[43]. The electronic configuration of each atom here is as follows: Rb: $4s^2\ 4p^6\ 5s^1$, Ge: $4s^2 4p^2$, I: $5s^2\ 5p^5$, Br: $4s^2 4p^5$, Cl: $3s^2 3p^5$. In the beginning, convergence calculations of the total energy ($E_{tolerance} = 2.7 \times 10 - 11$ eV) of the compounds have been done on Monkhorst–Pack mesh[44] of k-points and cut-off energy ($E_{cut-off}$). The Monkhorst–Pack special k-points were 6×6×6 for structural and electronic properties and set to 24×24×24 to calculate Eigen values and Eigen functions needed for optic properties calculations. The E_{tot} converged when $E_{cut-off}$ was 1235 eV. Full optimization for the structure dimensions has been performed for different pressures using PBE-GGA approach and (BFGS)[45, 46].

The lattice dimensions parameters and Wyckoff positions were obtained and used for later calculations. Band structure energies for all compounds are calculated employing PBG-GGA. As is well known, the PBE-GGA method underestimated the value of the band gap energy E_g when compared to the experimental values due to the strong fermion interactions in the heavy physical systems[47]. By performing DFPT, Eigen values and Eigen functions are obtained and used to calculate both the imaginary part and real part of frequency-dependent conductivity $\sigma(\omega)$:

$$\sigma(\omega) = \sigma_1(\omega) + i\sigma_2(\omega) \quad (1)$$

Where $\sigma_1(\omega)$ and $i\sigma_2(\omega)$ are real and imaginary parts of conductivity, respectively, and ω is frequency. The real part can be calculated using Kubo-Greenwood (KG) formulation[48]:

$$\sigma_1(\omega) = \frac{2\pi}{\Omega}\sum_{ij} F_{ij}\left|D_{ij}\right|^2 \delta\left(\epsilon_i - \epsilon_j - \omega\right) \quad (2)$$

Where Ω is atomic volume, F_{ij} is Fermi-Dirac distributions and ϵ is the dielectric function. And the imaginary part is calculated using Kramers-Kronig relations:

$$\sigma_2(\omega) = -\frac{2}{\pi} P\int \frac{\sigma_1(v)\omega}{(v^2-\omega^2)} dv \quad (3)$$

Where P is the principal value of the integral. The real part of the frequency-dependent dielectric response $\epsilon_1(\omega)$ and imaginary parts are calculated from imaginary and real parts of conductivity, respectively:

$$\epsilon_1(\omega) = 1 - \frac{4\pi}{\omega}\sigma_2(\omega) \quad (4)$$

$$\epsilon_2(\omega) = \frac{4\pi}{\omega}\sigma_1(\omega) \quad (5)$$

The total dielectric faction is the sum of the two parts and is related to the real part of the refractive index $n(\omega)$ and imaginary part $k(\omega)$ as follows:

$$\boldsymbol{\epsilon}(\omega) = \boldsymbol{\epsilon}_1(\omega) + i\boldsymbol{\epsilon}_2(\omega) = [n(\omega) + ik(\omega)]^2 \quad (6)$$

or

$$n(\omega) = \frac{1}{2}\sqrt{|\epsilon(\omega)| + \epsilon_1(\omega)} \quad (7)$$

$$k(\omega) = \frac{1}{2}\sqrt{|\epsilon(\omega)| - \epsilon_1(\omega)} \quad (8)$$

Refractive index components are related to the reflectivity $r(\omega)$ and absorption coefficient $\alpha(\omega)$ through the equations below:

$$r(\omega) = \frac{[1-n(\omega)]^2+k(\omega)^2}{[1+n(\omega)]^2+k(\omega)^2} \quad (9)$$

$$\alpha(\omega) = \frac{4\pi}{n(\omega)}\sigma_1(\omega) \quad (10)$$

3. Results and Discussions

3.1 Structural properties

The present research considers the ideal cubic of the $RbGeX_3$ (where X=I, Br, and Cl) perovskite which consists of a polyhedron that shares 12 halide atoms on the corners and is located inside the cube and one Rb atom in the body and 8 Ge atoms at the corners of the cube (figure 1). The unit cell contains one molecule of five atoms of Wyckoff positions as Rb 1b (0.5, 0.5, 0.5), Ge 1a (0.0, 0.0, 0.0), and X 3d (0.0, 0.0, 0.5).

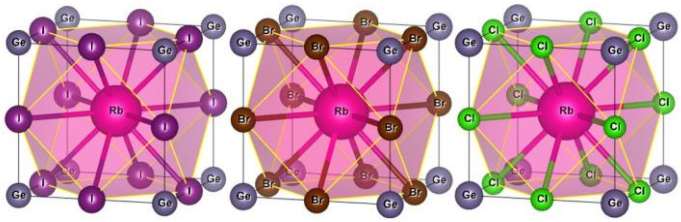

Figure 1: Ideal cubic structure of RbGeX3 (X= I, Br, and Cl).

Lattice constant (a), the bulk modulus (B), and its derivative (B') are calculated by fitting the change in energy (E_{tot}) as a function of varied volumes (V) by the Murnaghan-Birch equation of state as shown below[49, 50]:

$$E(V) = E_0 + \frac{9V_0B_0}{16}\left\{\left[\left(\frac{V_0}{V}\right)^{\frac{2}{3}} - 1\right]^3 B_0' + \left[\left(\frac{V_0}{V}\right)^{\frac{2}{3}} - 1\right]^2 \left[6 - 4\left(\frac{V_0}{V}\right)^{\frac{2}{3}}\right]\right\} \quad (11)$$

Where E_0 is the minimum energy of the compound and V_0 is the volume of the structure at minimum energy. The volume of the unit cell is plotted against E_{tot} (Figure 2). The calculated structural properties of $RbGeX_3$ (where X=I, Br, and Cl) are listed in table 1. Our values of calculated lattice constants are 5.95, 5.55, and 5.29 Å for $RbGeX_3$ (where X=I, Br, and Cl), respectively. Our values of a are in good agreement with available experimental values and other values except for the bulk modulus of $RbGeI_3$ where it is ~38 % larger, the advantage is to our result due to the reasonable variation trend of our results. Lattice parameter values show a decrement with an increment of the ionic radius of the halide dopant in the cell (i.e. ongoing from I to Cl) as in the case with other perovskite materials[51]. This may be, due to the strengthening covalent bonds between Ge and halide atoms[32]. The bulk modulus increases with decreased halogen ionic radii which indicates the material going through changing to more brittle materials ongoing from I to Cl.

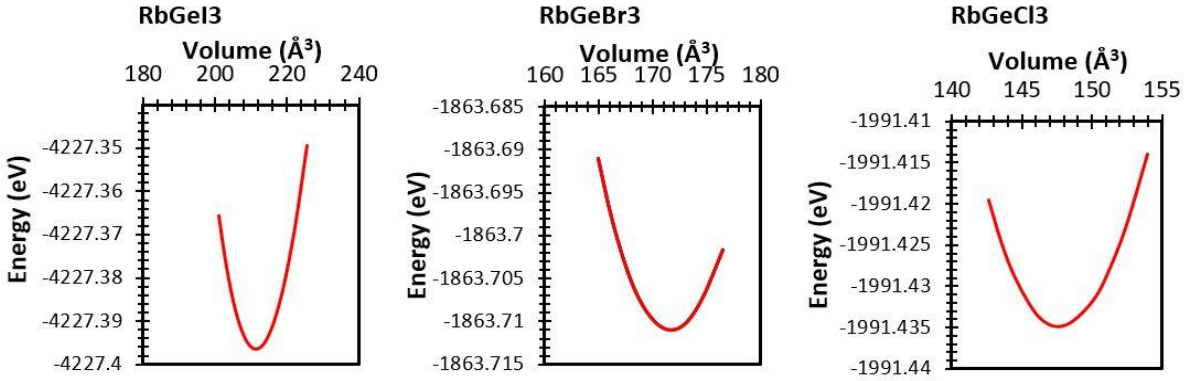

Figure 2: Total energy in eV as a function of volume in Å^3.

Tabel 1: Calculated lattice constant values (a), Bulk modulus (B), and its derivative (B') of cubic RbGeX3 (X= I, Br, and Cl).

Materials	a (Å)			B (GPa)		B' (GPa)	
	This work	Experimental	Other works	This work	Other work	This work	Other work
$RbGeI_3$	5.95	5.99a	5.96[b] 5.91[c]	17.76	12[b]	4.45	
$RbGeBr_3$	5.55		5.53[c] 5.57[d]	22.74	22.48[d]	4.31	4.14[d]
$RbGeCl_3$	5.29		5.27[c] 5.31[d]	26.71	26.15[d]	4.016	4.05[d]

3.2 Electronic properties

Band structure energies in electron volt of $RbGeX_3$ (where X=I, Br, and Cl) have been calculated using PBE-GGA approximation. Here, the first Brillouin zone (IBZ) and high symmetry k-points path Γ-X-M-R- Γ are chosen to represent band structure energies (Figure 3). The Fermi level is set to zero. Band structure shows that the compounds $RbGeX_3$ (where X=I, Br, and Cl) have the conduction band minimum (CBM) and valence band maximum (VBM) at R symmetry k-point (direct band gap value).

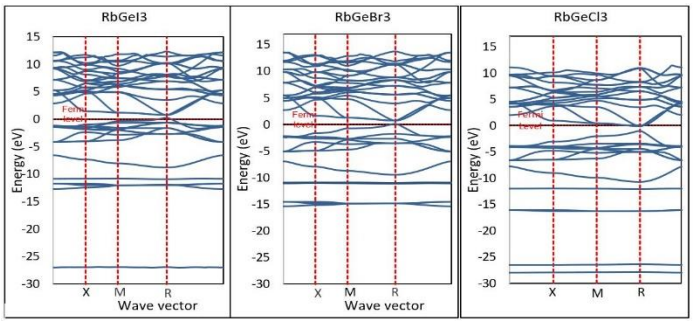

Figure 3: Band structure of $RbGeX_3$ (where X=I, Br, and Cl) compounds along high symmetry points path (Gamma-X-M-R-Gamma) using GGA approximation.

It is widely known that the PBE-GGA approximation underestimates the values of the E_g The resulting band gap energy values E_g from GGA approximation of the three halide perovskites of this work and other works results are listed in table 2. It is noted that results here comparably agree with other results which are also calculated using the GGA method. The band gap values are 0.53, 0.61, and 0.94 eV for $RbGeI_3$, $RbGeBr_3$, and $RbGeCl_3$, respectively. The E_g increases ongoing from I to Cl due to the weakening of the interaction of the electrons in the valence and conduction bands which depends on the number of electrons in both bands. These results show the tunable band gap characteristic of this group of perovskite materials as the halogen atom changes.

Tabel 2: Calculated band gap values (E_g) in eV $RbGeX_3$ (X= I, Br, and Cl) calculated in GGA approximation.

Materials		E_g (eV)	
		This work	Other works
$RbGeI_3$	GGA	0.53	
$RbGeBr_3$	GGA	0.61	0.67[a]
$RbGeCl_3$	GGA	0.94	0.96[a]

[a]reference[37],

To explain the CBM and VBM bands creation, the total and partial density of the state of $RbGeX_3$ (where X=I, Br, and Cl) compounds are calculated using GGA approximation and plotted as it is shown in figure 4. The valence state is created due to the contribution of the s states of the Ge and p states of the halogen atom and Ge atom. While the conduction band was created as the result of the contribution of the p states of the Ge and halogen (X) atoms. The hybridization of the p states of Ge and halogen atoms indicates the covalent nature of the bond between them.

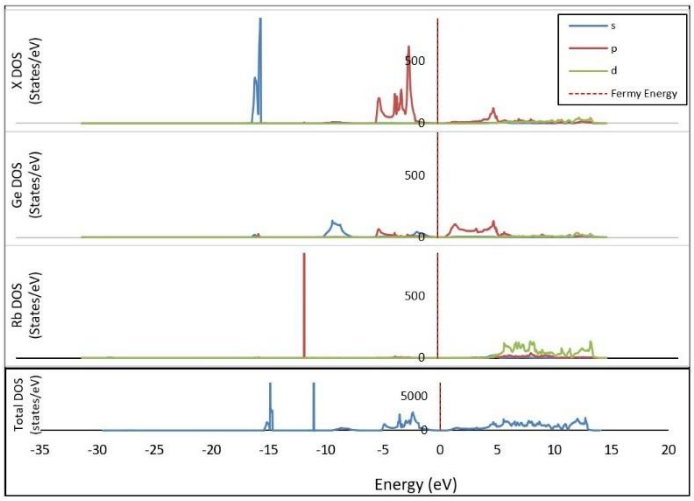

Figure 4: Total and partial density of states of the $RbGeX_3$ (where X=I, Br, and Cl) calculated using norm-conserving pseudopotentials in conjunction with GGA approximation.

3.3 Optical properties

The response of the cubic $RbGeX_3$ (where X=I, Br, and Cl) materials to electromagnetic radiation are investigated through computing dielectric function, absorption coefficient, and refractive index. The Eigen values and Eigen functions of the perturbed system are obtained using GGA approximation. These Eigen values and Eigen function are used to calculate the imaginary part of the dielectric function (Im(ε(ω))), the Real part of the dielectric function (Re(ε(ω))). As examples of both Im(ε(ω)) and Re(ε(ω)) parts, absorption coefficient α (m^{-1}) and refractive index are calculated.

The relationship between $Im(\varepsilon(\omega))$ and E_g value is obvious. It is shown in Figure 5a that the response of the three compounds $RbGeX_3$ (where X=I, Br, and Cl) is similar. The first transition (region I, fig.5a) happens from VBM to the CBM with represents the critical point and corresponds the E_g value. The response behavior can be explained in conjunction with DOS. The response of the $RbGeI_3$ is the highest because of the p state of the halogen contribution to the creation of the VBM and the iodine has the highest number of electrons. Region II is due to the transition of electrons between s state of Ge and d state of the Rb and the region III response appears as the result of transitions of the electron from s state of halogens and d state of the Rb element. It is also worth mentioning that the response shifts toward lower energies as the band gap decreases and the E_g value has an inverse relationship with Im(ε(ω)).

One of the other significant optical properties is the real part of the dielectric function Re(ε(ω)). Figure 5b shows the response of the Re(ε(ω)) to electromagnetic radiation ranging from 0 to 34 eV. The Re(ε(0)) response of the three compounds $RbGeX_3$ (where X=I, Br, and Cl) is very similar in pattern but different in values. The response starts to appear at zero frequency Re(ε(0)) at a certain point which represents the dielectric constant and increases to reach a maximum value at energies between 2 to 3 eV then decreases until it goes below 1 at energies ~7.5 to 9.3 eV. The dielectric constants of the three compounds are 7.21, 5.45, and 4.32 for $RbGeI_3$, $RbGeBr_3$, and $RbGeCl_3$, respectively.

The real part of the refractive index is also plotted here (Figure 5c), the behavior of the refractive index of the three compounds is similar to the Re(ε(0)). Except for the point where the $Re(n(0))$ starts to respond represents the actual refractive index value of the compound. The refractive index of the three compounds is 2.67, 2.33, and 2.07 for $RbGeI_3$, $RbGeBr_3$, and $RbGeCl_3$, respectively. The refractive index increases until reaches its maximum value at energies ranging between 3.32 to 2.38 eV then decreases until it goes below the unity of the three compounds at energies ranging from 9.63 to 14.6 eV because the phase velocity of the light becomes greater than the speed of light itself and these materials show the superluminality in this, particularly range of energy[52].

The absorption coefficient α (m^{-1}) starts to increase at energies in the infrared region until it reaches its maximum value at energies ranging from 18.9 to 20.04 eV for $RbGeX_3$ (where X=I, Br, and Cl) ongoing from I to Cl, $RbGeCl_3$ has the maximum value of α (m^{-1}) (2.07×10^8 m^{-1}) followed by $RbGeCl_3$ (1.87×10^8 m^{-1}) and $RbGeI_3$ (1.67×10^8 m^{-1}) (figure 5d).

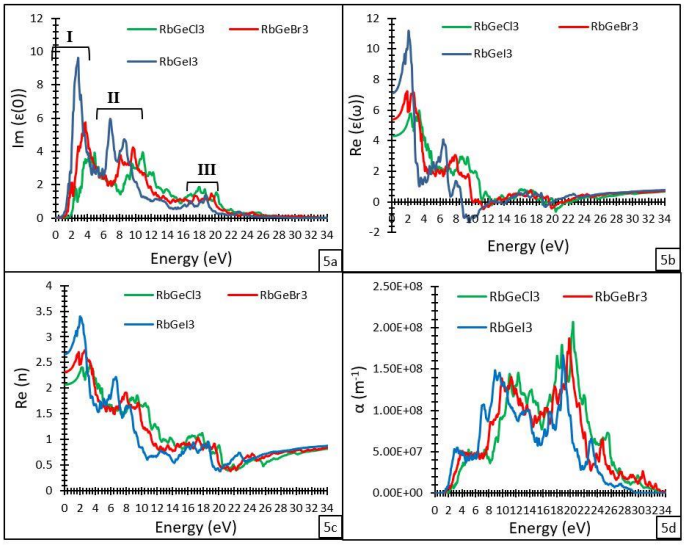

Figure 5: The imaginary part of the dielectric function (Im(ε(ω))), the Real part of the dielectric function (Re(ε(ω))), Im(ε(ω)) and Re(ε(ω)) parts and absorption coefficient α (m-1) of cubic $RbGeX_3$ (X=I, Br and Cl).

Conclusion

Structural, opto-electronic properties of ideal cubic and Pb-free $RbGeX_3$ (X=I, Br, and Cl) perovskite are carried out here using a

planewave-pseudopotential approximation in conjunction with the DFT framework. Lattice parameters obtained here are 5.95, 5.55, and 5.29 Å for $RbGeX_3$ (where X=I, Br, and Cl). Our values of a agree well with the available experimental values and other values except for the bulk modulus of RbGeI3 where it is ~38% larger, the benefit to our result due to the reasonable variance trend of our results. The lattice parameter values show a decrease with increasing ionic radius of the halide dopant in the cell (ie, from I to Cl). The band gap values are 0.53, 0.61, and 0.94 eV for RbGeI3, RbGeBr3, and RbGeCl3, respectively. The E_g increases from I to Cl due to the weakening of the interaction of the electrons in the valence and conduction bands, which depends on the number of electrons in both bands. These materials start to respond to the electromagnetic spectrum in the IR region and end at energy near 34 eV. $RbGeI_3$ is a better absorber and retainer to the radiation in low energies and $RbGeCl_3$ is a better absorber at medium and high energies. At the highest point where these materials can respond, $RbGeI_3$ has a better response again. Due to the lack of theoretical studies of these materials, and the absence, as to our knowledge, of experimental studies, more investigations needed to be done on these materials

Conflict of interests

None

Contribution

The author certifies that he has worked sufficiently in the work to take public responsibility for the content, including working on the concept, design, analysis, writing, or revision of the manuscript. Furthermore, the author certifies that this material or similar material has not been and will not be submitted to or published in any other publication before its appearance in the Passer journal of basic and applied science.

References

1. Castelli, I.E., et al., *Bandgap calculations and trends of organometal halide perovskites.* APL Materials, 2014. **2**(8): p. 081514.
2. Mao, X., et al., *First-principles screening of all-inorganic lead-free ABX_3 perovskites.* The Journal of Physical Chemistry C, 2018. **122**(14): p. 7670-7675.
3. Körbel, S., M.A. Marques, and S. Botti, *Stability and electronic properties of new inorganic perovskites from high-throughput ab initio calculations.* Journal of Materials Chemistry C, 2016. **4**(15): p. 3157-3167.
4. Tanaka, H., T. Oku, and N. Ueoka, *Structural stabilities of organic–inorganic perovskite crystals.* Japanese Journal of Applied Physics, 2018. **57**(8S3): p. 08RE12.
5. Tian, W., H. Zhou, and L. Li, *Hybridorganic–inorganic perovskite photodetectors.* Small, 2017. **13**(41): p. 1702107.
6. Stoumpos, C.C., et al., *Crystal growth of the perovskite semiconductor CsPbBr3: a new material for high-energy radiation detection.* Crystal growth & design, 2013. **13**(7): p. 2722-2727.
7. Dong, R., et al., *High-gain and low-driving-voltage photodetectors based on organolead triiodide perovskites.* Advanced materials, 2015. **27**(11): p. 1912-1918.
8. Song, J., et al., *Quantum dot light-emitting diodes based on inorganic perovskite cesium lead halides ($CsPbX_3$).* Advanced materials, 2015. **27**(44): p. 7162-7167.
9. Yoo, J.J., et al., *Efficient perovskite solar cells via improved carrier management.* Nature, 2021. **590**(7847): p. 587-593.
10. Zhao, Y. and K. Zhu, *Organic–inorganic hybrid lead halide perovskites for optoelectronic and electronic applications.* Chemical Society Reviews, 2016. **45**(3): p. 655-689.
11. Pellet, N., et al., *Mixed-organic-cation Perovskite photovoltaics for enhanced solar-light harvesting.* Angewandte chemie, 2014. **126**(12): p. 3215-3221.
12. Tiep, N.H., Z. Ku, and H.J. Fan, *Recent advances in improving the stability of perovskite solar cells.* Advanced Energy Materials, 2016. **6**(3): p. 1501420.
13. Zhang, Y., et al., *Direct-indirect nature of the bandgap in lead-free perovskite nanocrystals.* The Journal of Physical Chemistry Letters, 2017. **8**(14): p. 3173-3177.
14. Chen, L.-C., et al., *Enhanced efficiency of MAPbI3 perovskite solar cells with $FAPbX_3$ perovskite quantum dots.* Nanomaterials, 2019. **9**(1): p. 121.
15. Pan, Y., et al., *First-principles study on electronic structures of $FAPbX_3$ (X= Cl, Br, I) hybrid perovskites.* J. Adv. Nanomater, 2016. **1**(10.22606): p. 2016.
16. Govinda, S., et al., *Critical comparison of $FAPbX_3$ and $MAPbX_3$ (X= Br and Cl): How do they differ?* The Journal of Physical Chemistry C, 2018. **122**(25): p. 13758-13766.
17. Wang, H., et al., *Roles of organic molecules in inorganic $CsPbX_3$ perovskite solar cells.* Advanced Energy Materials, 2021. **11**(1): p. 2002940.
18. Nyayban, A., et al., *First principle studies of rubidium lead halides towards photovoltaic application.* Materials Today Communications, 2020. **24**: p. 101190.
19. Wang, M., et al., *Lead-free perovskite materials for solar cells.* Nano-Micro Letters, 2021. **13**(1): p. 1-36.
20. Xu, P., et al., *Influence of defects and synthesis conditions on the photovoltaic performance of perovskite semiconductor $CsSnI_3$.* Chemistry of Materials, 2014. **26**(20): p. 6068-6072.
21. Pecunia, V., et al., *Lead-free halide perovskite photovoltaics: Challenges, open questions, and opportunities.* APL Materials, 2020. **8**(10): p. 100901.
22. Noel, N.K., et al., *Lead-free organic–inorganic tin halide perovskites for photovoltaic applications.* Energy & Environmental Science, 2014. **7**(9): p. 3061-3068.
23. Giustino, F. and H.J. Snaith, *Toward lead-free perovskite solar cells.* ACS Energy Letters, 2016. **1**(6): p. 1233-1240.
24. Kamat, P.V., J. Bisquert, and J. Buriak, *Lead-free perovskite solar cells.* ACS Energy Letters, 2017. **2**(4): p. 904-905.
25. Wu, C., et al., *The dawn of lead-free perovskite solar cell: highly stable double perovskite $Cs_2AgBiBr_6$ film.* Advanced Science, 2018. **5**(3): p. 1700759.
26. Meng, X., et al., *Surface-controlled oriented growth of $FASnI_3$ crystals for efficient lead-free perovskite solar cells.* Joule, 2020. **4**(4): p. 902-912.
27. Soleimanpour, S. and F. Kanjouri, *Elastic, electronic and optical properties of the cubic fluoro-perovskite $KCaF_3$ under pressure.* Indian Journal of Physics, 2015. **89**(7): p. 687-697.
28. Amudhavalli, A., et al., *First-principles study of structural and optoelectronic properties of $CsSnI_3- yFy$ (y= 0, 1, 2, 3) perovskites.* Indian Journal of Physics, 2020. **94**(9): p. 1351-1359.
29. Ali, L., et al., *Theoretical studies of $CsSnX_3$ (X= Cl, Br and I) for energy storage and hybrid solar cell applications.* Materials Today Communications, 2020. **25**: p. 101517.
30. Rehman, J.U., et al., *First-principles calculations to investigate structural, electronics, optical and elastic properties of Sn-based inorganic Halide-perovskites $CsSnX_3$ (X= I, Br, Cl) for solar cell applications.* Computational and Theoretical Chemistry, 2022. **1209**: p. 113624.
31. Chen, L.-J., *Synthesis and optical properties of lead-free cesium germanium halide perovskite quantum rods.* RSC advances, 2018. **8**(33): p. 18396-18399.
32. Jong, U.-G., et al., *First-principles study on structural, electronic, and optical properties of inorganic Ge-based halide perovskites.* Inorganic chemistry, 2019. **58**(7): p. 4134-4140.
33. Hima, A. and N. Lakhdar, *Design and simulation of homojunction perovskite CH3NH3GeI3 solar cells.* Indian Journal of Physics, 2022: p. 1-5.

34. Stoumpos, C.C., et al., *Hybrid germanium iodide perovskite semiconductors: active lone pairs, structural distortions, direct and indirect energy gaps, and strong nonlinear optical properties.* Journal of the American Chemical Society, 2015. **137**(21): p. 6804-6819.

35. Yang, D., et al., *Germanium-lead perovskite light-emitting diodes.* Nature Communications, 2021. **12**(1): p. 1-7.

36. Krishnamoorthy, T., et al., *Lead-free germanium iodide perovskite materials for photovoltaic applications.* Journal of Materials Chemistry A, 2015. **3**(47): p. 23829-23832.

37. Houari, M., et al., *Semiconductor behavior of halide perovskites $AGeX_3$ (A= K, Rb and Cs; X= F, Cl, and Br): first-principles calculations.* Indian Journal of Physics, 2020. **94**(4): p. 455-467.

38. Parrey, K.A., et al., *First principle studies on structure, magneto-electronic and elastic properties of photovoltaic semiconductor halide ($RbGeI_3$) and ferromagnetic half metal oxide (RbDyO3).* Computational Condensed Matter, 2019. **19**: p. e00381.

39. Honenberg, P. and W. Kohn, *Inhomogeneous electron gas.* RESONANCE-JOURNAL OF SCIENCE EDUCATION, 2017. **22**(8): p. 810-811.

40. Sham, L.J. and W. Kohn, *One-particle properties of an inhomogeneous interacting electron gas.* Physical Review, 1966. **145**(2): p. 561.

41. Collins, L., et al., *Dynamical and optical properties of warm dense hydrogen.* Physical Review B, 2001. **63**(18): p. 184110.

42. Gonze, X., et al., *ABINIT: First-principles approach to material and nanosystem properties.* Computer Physics Communications, 2009. **180**(12): p. 2582-2615.

43. Krack, M., *Pseudopotentials for H to Kr optimized for gradient-corrected exchange-correlation functionals.* Theoretical Chemistry Accounts, 2005. **114**(1): p. 145-152.

44. Monkhorst, H.J. and J.D. Pack, *Special points for Brillouin-zone integrations.* Physical Review B, 1976. **13**(12): p. 5188.

45. Perdew, J., K. Burke, and M. Ernzerhof, *Perdew, burke, and ernzerhof reply*. Physical Review Letters, 1998. **80**(4): p. 891.

46. Head, J.D. and M.C. Zerner, *A Broyden—Fletcher—Goldfarb—Shanno optimization procedure for molecular geometries.* Chemical physics letters, 1985. **122**(3): p. 264-270.

47. Perdew, J.P., et al., *Accurate density functional with correct formal properties: A step beyond the generalized gradient approximation.* Physical review letters, 1999. **82**(12): p. 2544.

48. Harrison, W., *Solid State Theory McGraw-Hill.* New York London Toronto, 1970.

49. Birch, F., *Finite elastic strain of cubic crystals.* Physical Review, 1947. **71**(11): p. 809.

50. Murnaghan, F.D., *The compressibility of media under extreme pressures.* Proceedings of the National Academy of Sciences, 1944. **30**(9): p. 244-247.

51. Verma, A. and V. Jindal, *Lattice constant of cubic perovskites.* Journal of alloys and compounds, 2009. **485**(1-2): p. 514-518.

52. Babu, K.E., et al. *Investigation of optoelectronic properties of cubic perovskite $LaGaO_3$.* in *AIP Conference Proceedings*. 2014. American Institute of Physics.